Nuclear Instruments and Methods in Physics Research A 370 (1996) 429–434

ELSEVIER

NUCLEAR INSTRUMENTS & METHODS IN PHYSICS RESEARCH Section A

Measurement of the response of long plastic scintillator bars for the large angle electromagnetic shower calorimeter for CLAS

M. Taiuti[a,*], P. Rossi[b], R. Morandotti[a,1], M. Anghinolfi[a], H. Avakian[b], M. Battaglieri[a], N. Bianchi[b], P. Corvisiero[a], E. DeSanctis[b], V. Giourjian[b], P. LeviSandri[b], A. Longhi[a], V.I. Mokeev[c], V. Muccifora[b], M. Olcese[a], E. Polli[b], A.R. Reolon[b], G. Ricco[a], M. Ripani[a], M. Sanzone[a], A. Zucchiatti[a]

[a] *Dipartimento di Fisica dell'Università di Genova or INFN – Sezione di Genova, I-16146, Genova, Italy*
[b] *INFN – Laboratori Nazionali di Frascati, P.O. Box 13, I-00044, Frascati, Italy*
[c] *Institute of Nuclear Physics, Moscow State University, Moscow, Russian Federation*

Received 12 June 1995; revised form received 5 September 1995

Abstract

The behaviour of plastic scintillator bars with length up to 450 cm, designed for the CLAS large angle electromagnetic shower calorimeter, is considered in relation to the overall calorimeter response function. In particular methods adopted to measure the light emission yield and transmission efficiency are described and the influence of the scintillator bar properties on the calorimeter energy read-out and timing is discussed. We found that the new scintillator NE110A manufactured by NE Technology Ltd. showed the best agreement with our demands. The effect of wrapping materials on the scintillator bar properties has been studied considering also the temperature variations expected in Hall B at CEBAF.

1. Introduction

The AIACE collaboration [1] participates to the CEBAF [2] Hall B experimental activity. Hall B is equipped with a large angle spectrometer (CLAS) [3] based on a toroidal magnetic field. The field is generated by six super-conducting coils arranged around the beam line to produce a magnetic field that is primarily in the ϕ-direction. Each region between two coils is equipped with a) three layers of drift chambers to track the charged particle, b) a Cherenkov detector to discriminate electrons from pions, c) scintillator counters for time-of-flight measurements and d) an electromagnetic calorimeter to detect electrons and photons. The AIACE collaboration will provide the modules of the electromagnetic shower calorimeter (AIACE-ESC) to detect particles at angles larger than 45° in the laboratory. The ESC is used for a) the π/e separation, b) the detection of photons from the decay of mesons (π^0, η, η'...), c) the measurement of neutron momentum using time-of-flight.

Different technologies were adopted to realise electromagnetic calorimeters with large angle acceptance: a) BGO crystals as for L3 [4], b) lead glasses as for the detectors of E760 experiment [5] or OPAL [6], c) towers of scintillating fibres embedded in a lead bulk as in the SPACAL detector [7], d) lead and liquid argon as for the detector of NA31 experiment [8], e) multi-layer structure made by lead sheets and scintillator bars as for the electromagnetic calorimeter in CLAS [9]. The AIACE-ESC modules are based, like the forward ESC, on the last configuration that provides the best agreement between good energy resolution and high neutron detection efficiency requirements. Each module consists of 33 layers, each composed by a lead foil with thickness 0.20 cm and plastic scintillator bars with average width 10 cm and constant thickness 1.5 cm. Each layer is rotated by 90° to form a 40×24 matrix of $\approx 10 \times 10$ cm^2 cells. The bar width increases going from the inner side toward the outer to guarantee the tapering required by the CLAS geometry. The surface exposed to particle fluxes is 217×400 cm^2. The module is vertically divided into an inner and an outer part to improve the electron–pion discrimination. Scintillators lying (for the inner and outer part separately) one on top of the other with the same orientation form 128 different stacks. In Fig. 1 a conceptual drawing of the calorimeter shape and its internal structure is reported. The electromagnetic showers originate in the lead sheets and propagate through the layers; the energy absorbed in the active material produces a light pulse that is collected at both

* Corresponding author.

[1] Present address: NE Technologies, Edinburgh, Scotland.

SSDI 0168-9002(95)00848-9

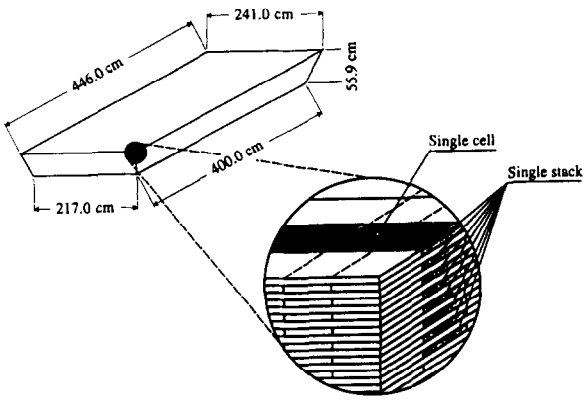

Fig. 1. Conceptual drawing of the calorimeter volume showing in detail the plastic scintillators stack structure (light gray area) and the crossing of two orthogonal stacks that defines a cell (dark gray area).

scintillator ends. The collected light is summed, separately for each stack, before the photomultiplier. Therefore light pulses emitted from eight different scintillators are summed up on a single photomultiplier that is placed on the top surface of the AIACE-ESC module several centimetres away from the scintillators.

Monte Carlo simulations showed that the AIACE-ESC performance is strongly affected by the scintillator bar properties: in particular the light attenuation makes the AIACE-ESC response function position-dependent providing better resolution and timing for particles detected close to the module edges. Monte Carlo simulations showed also that, even if a software position correction procedure improves homogeneity, a light attenuation length longer than 300 cm is necessary to reduce corrections down to 5%. Fluctuations around average values also affect the energy resolution. Handling and ageing of scintillator bars can also spoil their performance.

The measurement of scintillator bar properties was then necessary to identify the best material to be used. We considered the following properties: a) light output, b) light transmission and c) timing. Experimentally properties a) and c) are normally convoluted with the photomultiplier response function. Transmitted light shows as general behaviour an exponential trend with a long λ_0 and a short λ_1 attenuation length components described by the expression

$$A(x) = A_0 e^{-x/\lambda_0} + A_1 e^{-x/\lambda_1}, \quad (1)$$

with λ_1 being of the order of a few centimetres and λ_0 ranging from 1 to several meters. The relative weight A_1/A_0 strongly depends on the adopted read-out system.

In this paper we report on the results from scintillator prototypes produced by NE Technology and the comparison with standard BICRON and NE Technology scintillators. Scintillators were measured with and without wrapping and the effect of temperature variations is also discussed.

2. The testing apparatus

We tested the scintillator bars using the device described in Ref. [10] and a collimated 100 μCi ^{90}Sr β-source ($E_{max} = 2.27$ MeV). The maximum energy released in plastic scintillators 1.5 cm thick by the ^{90}Sr β-electrons corresponds to the energy released by a minimum ionising particle in the same material and to the average energy (Mee units) deposited by interacting neutrons. To select the high energy part of the β spectra we tested the scintillator bars without any wrapping using a fast Hamamatsu R1828-01 trigger photomultiplier (TP) placed in front of the source on the other side of the scintillator. This photomultiplier provided an energy and a timing trigger for the acquisition of signals from the analysing photomultiplier (AP) EMI 9954B equal to those chosen for the AIACE-ESC module. We used two different settings for the AP High Voltage: a) for light output measurements the gain was set to 100 pC/MeV to cover the ADC range, while b) for timing measurements it was set to 6 pC/MeV to reproduce the experimental configuration where a charge of 1400 pC corresponds to the maximum deposited energy in one stack (≈350 MeV). The AP photomultiplier was coupled to one scintillator end in different ways: a) directly in air b) with a lucite light guide and optical grease between the photomultiplier and the light guide or c) with optical fibres. The AP spectra, with a TP energy threshold corresponding to 2 MeV, showed a gaussian shape with a ratio amplitude/sigma roughly proportional to the square root of the number of collected photo-electrons. The timing and energy triggers have been obtained using a CAEN N413 octal 150 MHz leading edge discriminator with minimum threshold −20 mV. The source and the trigger photomultiplier are placed on a sliding frame moved by a computer controlled stepping motor. We measured the light transmission by 22.5 cm steps starting 10 cm from the scintillator edge coupled to AP. For each measure the average charge and timing were evaluated together with their variances. To reproduce the real configuration of scintillators inside the module the end of the scintillator opposite to the coupling with the photomultiplier was not blackened. In Fig. 2 a conceptual drawing of the testing apparatus and acquisition logic is reported. The whole apparatus is mounted in a light tight wooden box $70 \times 40 \times 600$ cm^3; the box is equipped with an internal copper tube 1 cm diameter 27 m long running along the internal walls and filled with recirculating water and connected to an external thermostat. The box temperature can range from 5°C to 35°C.

3. The scintillators properties

We studied many samples obtained from BICRON and NE Technology. Although BICRON scintillators chosen for the CLAS forward angle calorimeter satisfied our

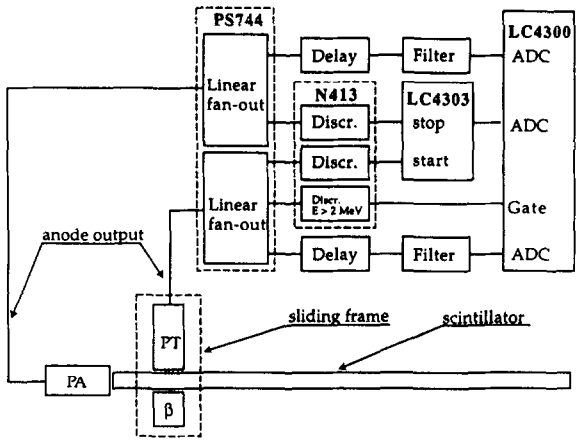

Fig. 2. The experimental setup.

requests, we focused our interest on the new NE Technology product NE110A especially developed for the AIACE project. We received two samples with cross section 100 × 15 mm^2 and length 382 and 400 cm respectively. These scintillator bars showed a very long attenuation length with absolute light output and timing comparable to those of previous scintillators.

3.1. The light output and transmission

In Fig. 3 the average charge collected by photomultiplier AP is reported as a function of the β-source position. The two NE110A samples showed, with AP directly coupled, an attenuation length equal to 336±7 cm and 481±12 cm respectively and higher than the lowest acceptable limit (300 cm) for the AIACE scintillators defined by Monte Carlo simulations. Only the long component has been detected, being the short one probably depressed by the photomultiplier coupling configuration, and data were fitted with a single exponential with the form

$$F(x) = C_0 e^{-x/\lambda}. \quad (2)$$

In the same figure the results of the measurement of BC412 and previous NE110 samples are reported for comparison. Referring to the NE110 sample the two prototypes show a larger attenuation length that compensates for the generally lower NE absolute light output compared to BC412.

The single measurements for both NE110A samples differ from the fitting function by less than ±5% as reported in Fig. 4a with a standard deviation of 2.5%. The main feature is however a waving deviation from the single exponential fit that originates from a relative increase in collected light as the source approaches the opposite end of the scintillator. This effect could be explained observing that a fraction α of the emitted light

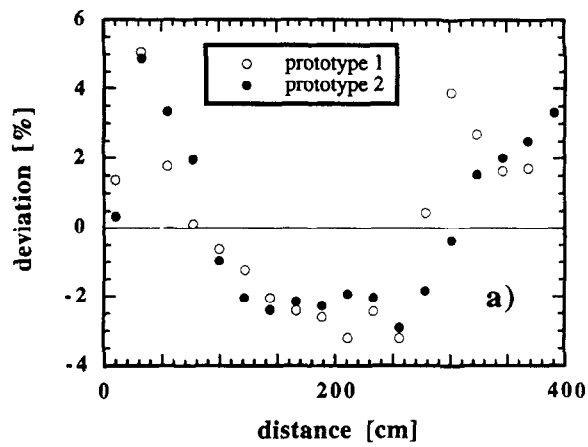

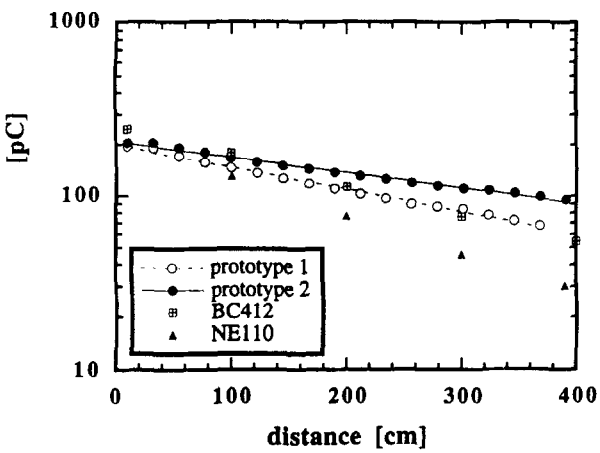

Fig. 3. The light transmission for scintillators NE110A (dots), NE110 (triangles) and BC412 (squares) with the photomultiplier AP directly coupled (errors are within the symbol size).

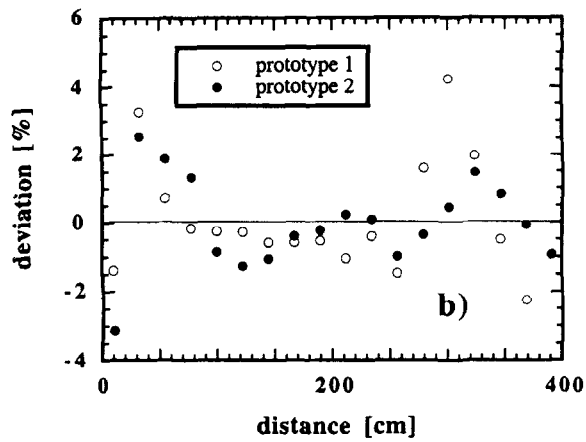

Fig. 4. The deviation of light transmission for NE110A scintillators from (a) an exponential fit and (b) an exponential fit with correction for the reflected light contribution.

could be reflected back to the photomultiplier adding to the direct light a second component as described by the simple expression

$$G(x) = C_0(e^{-x/\lambda} + \alpha e^{-(2L-x)/\lambda}). \quad (3)$$

With the new fit the waving behaviour almost disappears as shown in Fig. 4b and the standard deviation reduces to 1.5%.

The same measurements were performed using a lucite light guide similar to those adopted for the AIACE-ESC modules. [11] The light output is reduced by a factor of about 8 but shows the same position dependence measured in direct coupling. The results are reported in Fig. 5 for the first prototype.

In the AIACE-ESC modules the scintillator light is collected separately at both ends (called l and r in the following equation) and the simple behaviour described by Eq. (2) would permit to extract the deposited energy by means of the following expression

$$E \propto \sqrt{F_l(x)F_r(x)} = C_0\sqrt{e^{-x/\bar{\lambda}}e^{-(L-x)/\bar{\lambda}}} = C_0 e^{-L/2\bar{\lambda}}, \quad (4)$$

with being L the scintillator length and $\bar{\lambda}$ the effective attenuation length of the scintillator stack. The deviation of the value E of the reconstructed energy obtained with Eq. (4) from the actual value obtainable from the product $\sqrt{G_l(x)G_r(x)}$ for the two prototypes is of the order of 2–3%, smaller than the estimated energy resolution.

3.2. The timing

We also analysed the timing spread studying in particular the effect of the light propagation (σ_x) as a function of the light emission point. We used, as previously described, an experimental setup that provided an almost constant light output. However the light propagation affected the intensity of the transmitted light summing to (σ_x) the contributions of photo-electron fluctuations ($\sigma_{p.e.}$) that had to be measured separately.

The photo-electron fluctuations $\sigma_{p.e.}$ were obtained fixing the source position at 10 cm in order to minimise the contribution of the position dependence σ_x and moving the photomultiplier AP far from the scintillator thus reducing the solid angle. However, the very low gain made the measurement very sensitive to the jitters generated by the Leading Edge Discriminator and a software correction was necessary to extract $\sigma_{p.e.}$. The results are reported in Fig. 6a and shows the timing fluctuations as a function of the charge before any pulse height correction. The points were fitted with the expression

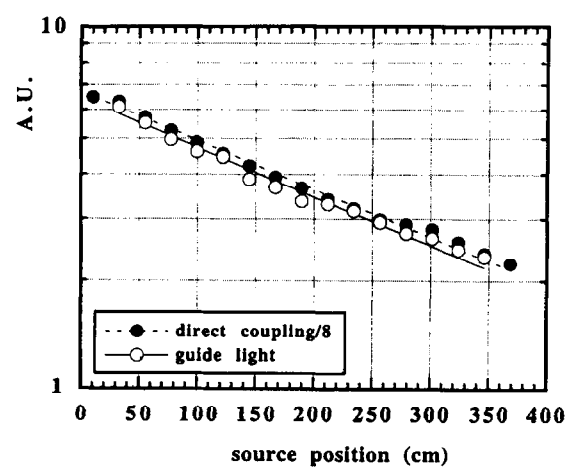

Fig. 5. The light transmission for NE110A prototype 1 with the photomultiplier AP coupled by a lucite light guide (errors are within the symbol size).

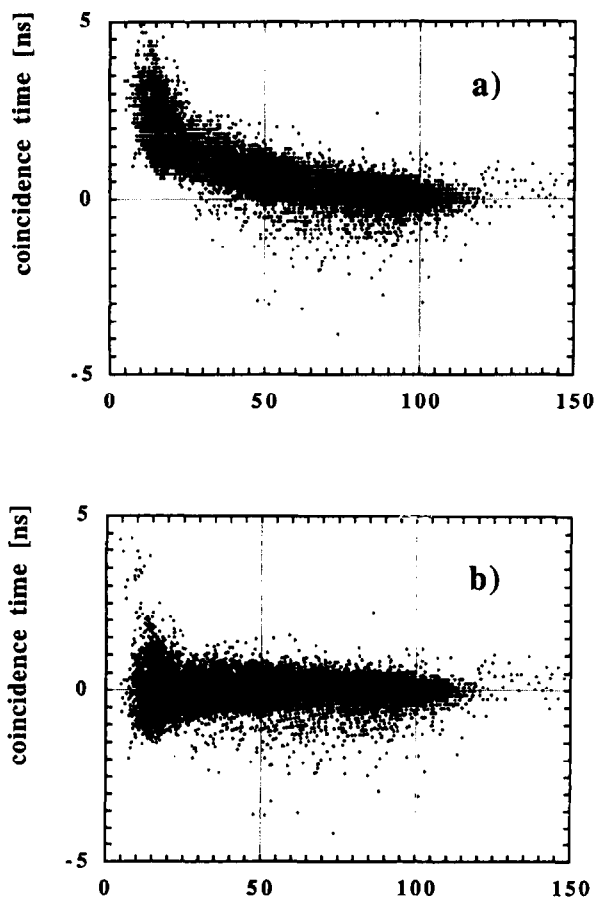

Fig. 6. The charge dependence of the timing response without (a) and with (b) the software correction for the discriminator jitters. Points represent six different measurement sets corresponding to different AP positions and each set is plotted alternatively using empty or full dots.

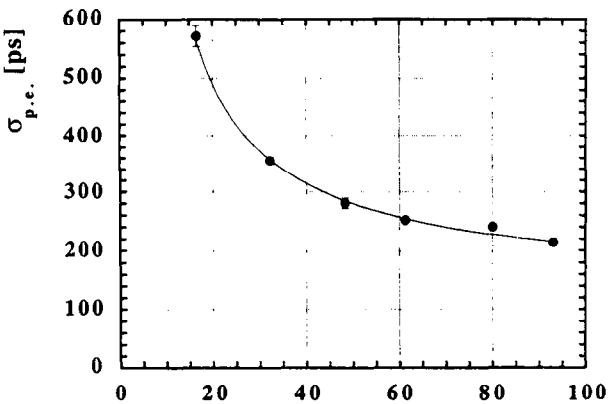

Fig. 7. The charge dependence of the $\sigma_{p.e.}$ timing resolution.

$$t' = t - 3.79e^{-\langle q\rangle/28} \quad [\text{ns}], \tag{5}$$

with $\langle q\rangle$ the average charge in pC for each measurement. Fig. 6b shows the same measurements after the correction. The two plots show the overlapping of six different measurements always obtained selecting by the PT threshold the same high energy tail of the β-source energy distribution. The charge dependence of $\sigma_{p.e.}$ is reported in Fig. 7 for the corrected distribution for each measurement and fitted with the expression

$$\sigma_{p.e.} = 140 + \frac{7\times 10^3}{\langle q\rangle} \quad [\text{ps}]. \tag{6}$$

The contribution of light propagation (σ_x) to the timing spread has been extracted as a function of x from the measured σ_t values through the expression

$$\sigma_x = \sqrt{\sigma_t^2 - \sigma_{p.e.}^2}, \tag{7}$$

using for $\sigma_{p.e.}$ the values corresponding to the measured average charge.

The procedure is reported in Fig. 8 where the measured σ_t and $\sigma_{p.e.}$ together with their fit and the resulting σ_x trend are reported. It resulted that the timing properties become sensitive to the position for distances higher than 200 cm where the contribution is higher than 200 ps and the behaviour is fairly well described by

$$\sigma_x = 530(e^{x/590} - 1) \quad [\text{ps}], \tag{8}$$

with x in cm.

4. The wrapping material properties

The experimental apparatus has been used to study the performance of scintillator bars when wrapped or subjected to temperature variations.

We tested four different materials: aluminised Mylar®, Teflon®, Tyvek® and NE adhesive paper. We wrapped the scintillators making on the wrapping material 4 cm diameter holes to provide optical coupling between the scintillator and the TP photomultiplier. In Fig. 9 the results are compared with the bare scintillator performance. The first three materials do not appreciably affect the transmitting properties with only a slight improvement for the Tyvek while the NE adhesive paper reduces the transmission efficiency, this effect being due to the change in the total reflection angle. We had to exclude Tyvek because its surface roughness could under pressure modify the scintillator surface affecting the light reflection [12].

Then we uniformly loaded the wrapped scintillator with 56 g/cm^2 pressure corresponding to the average load in the module and cycled twice the temperature from 23°C to 32°C. The scintillator (prototype 1) wrapped with aluminised Mylar showed a strong permanent reduction in the

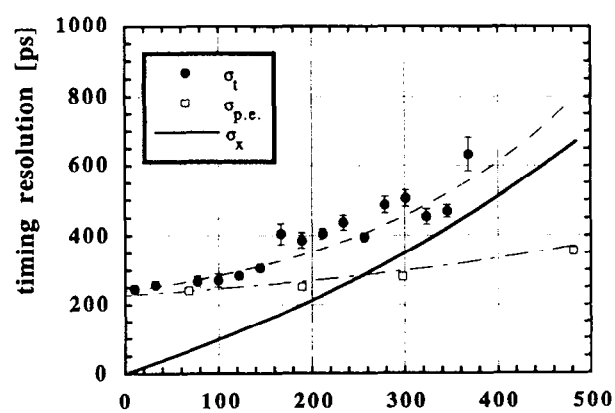

Fig. 8. The scintillator timing resolution (– – • – –) with charge $\sigma_{p.e.}$ (– · – □ – · –) and position σ_x (———) contributions.

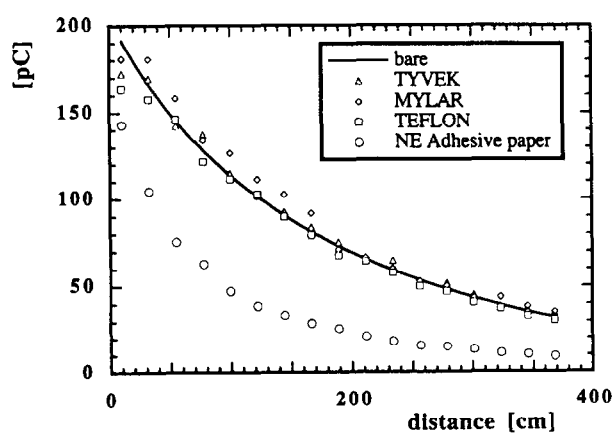

Fig. 9. The effect of wrapping material on the light transmission for different materials (errors are within the symbol size).

attenuation length, while that (prototype 2) wrapped with Teflon showed no appreciable variations in the attenuation length.

These measurements were performed one year ago and prototype 2 has been continuously used, since last year, to perform tests on the collecting light systems and photomultipliers. Nevertheless prototype 2 has not shown any appreciable change from the initial measured properties.

5. Conclusions

We measured the response of long plastic scintillator bars (400 cm) that will be used for the active part of the sampling AIACE-ESC detector. The scintillator response has been studied considering that the light will be collected at both ends by means of light guides. We measured a) the light output, b) the light transmission and c) the timing with a testing apparatus that reproduced the experimental conditions. A ^{90}Sr β-source has been used to simulate minimum ionising particles and interacting neutrons.

The new plastic scintillator bars showed an absolute light output comparable to that of previous scintillators like NE110 and BC412 coupled to a very good attenuation length, higher than NE110 and comparable to BC412. The timing properties were studied as a function of a) the number of photoelectrons and b) the emission point separately. Photoelectrons contribute with a $1/q$ dependence while the position dependence showed a divergent exponential behaviour that dominates at distances higher than 200 cm.

The effect of wrapping material on the scintillator performance has been also investigated studying the light transmission properties. Teflon showed the best agreement with our constraints. In particular it does not affect the light transmission or modify the scintillator surface with uniform loading up to 56 g/cm^2.

Acknowledgments

We would like to thank the CEBAF staff for the fruitful discussions on the scintillator measurement results. In particular V. Burkert and S. Majewski for the wrapping materials, Yu. Efremenko and S. Stepanyan for the experimental setup.

We gratefully acknowledge the technical staff of the Genova (M. Castoldi, P. Cocconi, F. Parodi and A. Rottura) and Frascati (M. Albicocco) groups for the continuing assistance in all stages of the apparatus construction and scintillator tests.

References

[1] M. Anghinolfi et al., Proc. Int. Workshop on Flavour and Spin in Hadronic and Electromagnetic Interactions, Torino, Italy, September 21–23, 1992, eds. F. Balestra, R. Bertini and R. Garfagnini, Ital. Phys. Soc. 39 (1993) p. 237.
[2] J.J. Domingo, Proc. 5th Workshop on Perspectives in Nuclear Physics at Intermediate Energies, Trieste, Italy, May 6–10, 1991, eds. S.Boffi, C.Ciofi degli Atti and M.Giannini (World Scientific, 1992) p. 260.
[3] V.D. Burkert and B.A. Mecking, Modern Topics in Electron Scattering, eds. B. Frois and I. Sick (World Scientific, 1991).
[4] J.A. Bakken et al., Nucl. Instr. and Meth. A 254 (1987) 535.
[5] L. Bartoszek et al., Nucl. Instr. and Meth. A 301 (1991) 47.
[6] M.A. Akrawy et al., Nucl. Instr. and Meth. A 290 (1990) 76.
[7] D. Acosta et al., Nucl. Instr. and Meth. A 308 (1991) 481.
[8] H. Burkhardt et al., Nucl. Instr. and Meth. A 268 (1988) 116.
[9] Conceptual Design Report – Basic Experimental Equipments, CEBAF, April 13, 1990.
[10] M. Taiuti et al., INFN-GE Report TC-94/08 (1994).
[11] M. Taiuti et al., Nucl. Instr. and Meth. A 357 (1995) 344.
[12] NE Technology Ltd., private communication.